
Chapter 3

Experimental Methods and Procedures

3.1 Processing of Ceramic Powder

In this study, the two types of lead zirconate titanate (PZT) were used for the ceramic filler or dispersed phase. The type 40/30 PZT powder (from Advanced Ceramic Limited) has been widely used commercially. Another type was the $\text{Pb}(\text{Zr}_{0.52}\text{Ti}_{0.48})\text{O}_3$ powder which was prepared by conventional mixed oxide method.

3.1.1 The Commercial 40/30 PZT Powder

The commercial 40/30 PZT powder (prepared by spray drying method) was ball-milled in ethanol for 24 hours. Then it was stirred, dried and calcined at 1200 °C for 2 hours with heating/cooling rate of 5 °C/min in a closed alumina crucible. The calcined powder was sieved through

mesh number 100 and 300 to separate the particle sizes. This powder was employed to prepare the (0-3) composites.

The schematic diagram of powder preparation is shown in Figure 3.1. The particle distribution of the powder was scanned using a Shimazu sedimentrograph (analysette 22).

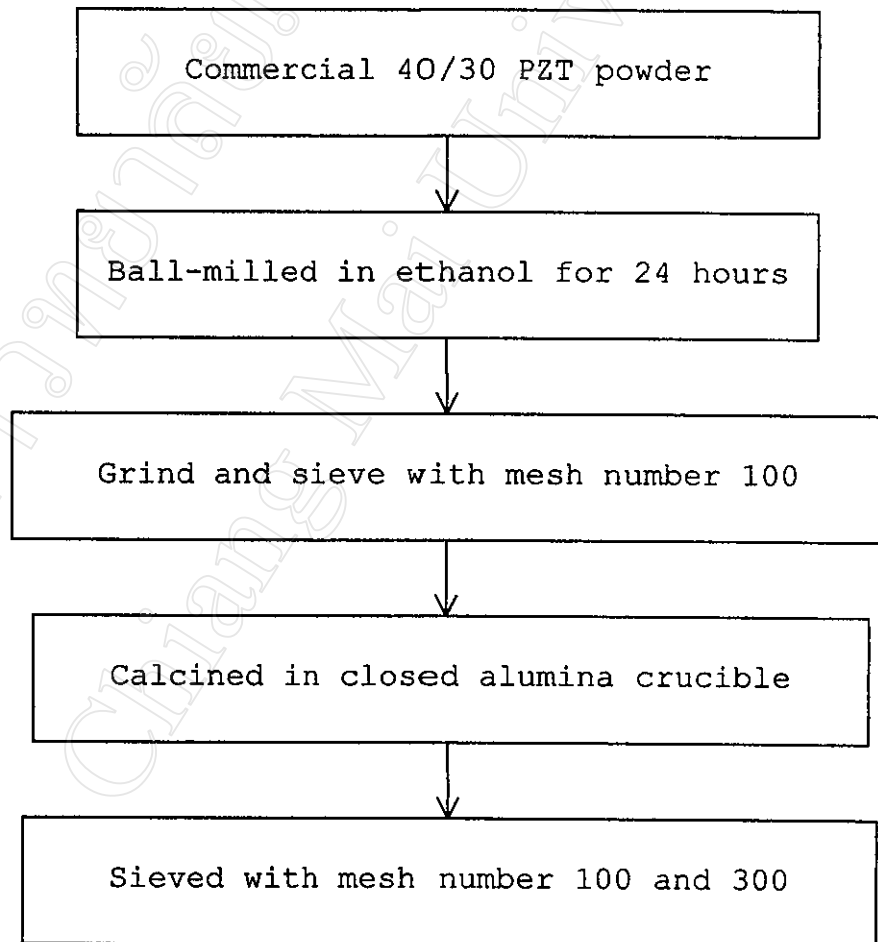


Figure 3.1 Schematic diagram of preparing the commercial 40/30 PZT powder.

3.1.2 The $\text{Pb}(\text{Zr}_{0.52}\text{Ti}_{0.48})\text{O}_3$ Mixed Oxide Powder

The precursors, lead oxide (PbO), zirconium oxide (ZrO_2) and titanium dioxide (TiO_2) were thoroughly mixed and milled in ethanol for 24 hours. After that, the mixed powder was stirred, dried and calcined in closed alumina crucible at temperature $1200\text{ }^\circ\text{C}$ for 2 hours with heating/cooling rate as $5\text{ }^\circ\text{C}/\text{min}$. The powder was sieved with mesh number 100 to separate the particle sizes. The distribution of particle size was scanned using a sedimentograph. Figure 3.2 shows a schematic diagram of powder preparation. Thereafter, the PZT powder was prepared to composites by centrifuge technique as described in the later section.

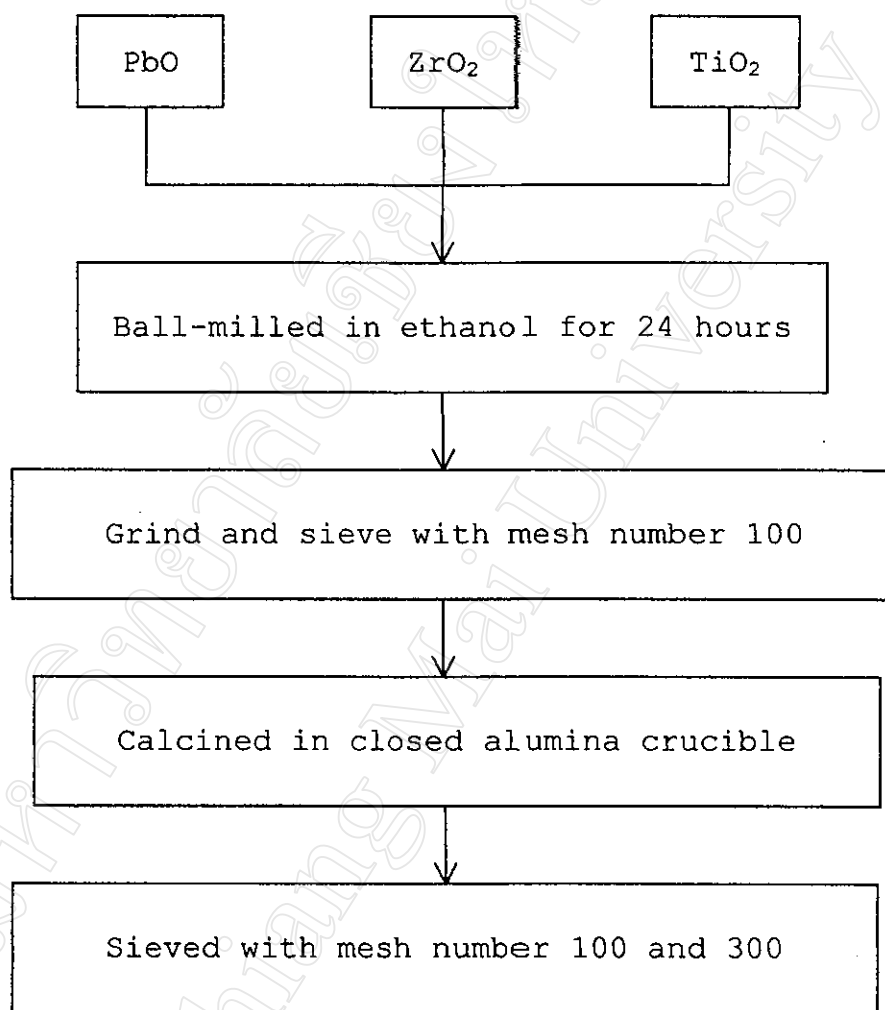


Figure 3.2 Schematic diagram of preparing of $\text{Pb}(\text{Zr}_{0.52}\text{Ti}_{0.48})\text{O}_3$ mixed oxide powder.

3.2 Processing of 0-3 ceramic-polymer composites

Ceramic-polymer composites with 0-3 connectivity were fabricated using the conventional method, using a calender, and the centrifuge method. The PZT powder obtained from mixed oxides following subsections was mixed with polyethylene (PE) on two hot rolling drums of a calender. The powder obtained from 40/30 PZT powder was mixed with polyester resin for a centrifuge.

3.2.1 Conventional Method

In this method, a calender was employed to fabricate the 0-3 ceramic-polymer composites. Various volumetric fractions of the ceramic powder and polyethylene were mixed on two hot-rolling drums of a calender. The composite sheets were rolled in a calender for several times to obtain a well distributed of ceramic powder in the composite sheets. However, this method is rather difficult to load ceramic powder in polymer phase more than 50 volume%. Mixing in a centrifuge was introduced for a better result. The PZT powder and PE were prepared in ratios of 40, 50 and 60 volume%. Each of them was put into

hot xylene (about 100 °C) and stirred until all of PE was totally dissolved. The xylene solution at this stage was completely volatile. After that, the mixture was pressed in the hot-rolling drums of the calender at the temperature of 150 °C for 1 hour when it became consolidated. Next, the mixture was pressed in a hot hydraulic press and then became composite sheets with thickness of 0.5 mm. The temperature of the hot-press was 150 °C, and the pressing time was 8 minutes. Finally, the sheets of the composites were punched into disc shape with radius of 0.5 inch. The surfaces of the samples were polished with a fine (1000 grit) silicon carbide emery paper.

3.2.2 Centrifuge Method

Although the conventional method is simple and can be adapted for mass production, a new processing technique is required to produce the composites with uniform microstructure and higher ceramic powder percentages. Furthermore, it should be simple, easy and able to produce mass product. In the present study, a centrifuge has been

developed for the production of highly homogeneous ceramic-polymer composites of 0-3 type¹. The procedure of the centrifuge method was shown in Figure 3.3. The main procedures include following steps.

- (1) The PZT powder was mixed into polyester resin.
- (2) About 2 cm³ of the samples which were slurry at the moment, were put into plastic tubes of about 1 cm in diameter.
- (3) The powder was spun in a centrifuge with a speed of 4500 rpm for 30 minutes.
- (4) The samples were left for few minutes to settle.
- (5) The rod of samples were cut in disc shape with thickness of 1 mm and 0.5 mm.
- (6) The composites samples were polished with a fine silicon carbide emery paper and very fine alumina powder.

The kind of polymer which used for matrix phase is polyester resin (WINSON SCREEN CO.,LTD.). The PZT powder prepared from solid state mixed oxide [Pb(Zr_{0.52}Ti_{0.48})O₃] and 40/30 PZT (Advanced-Ceramic Limited) were used for the dispersed phase.

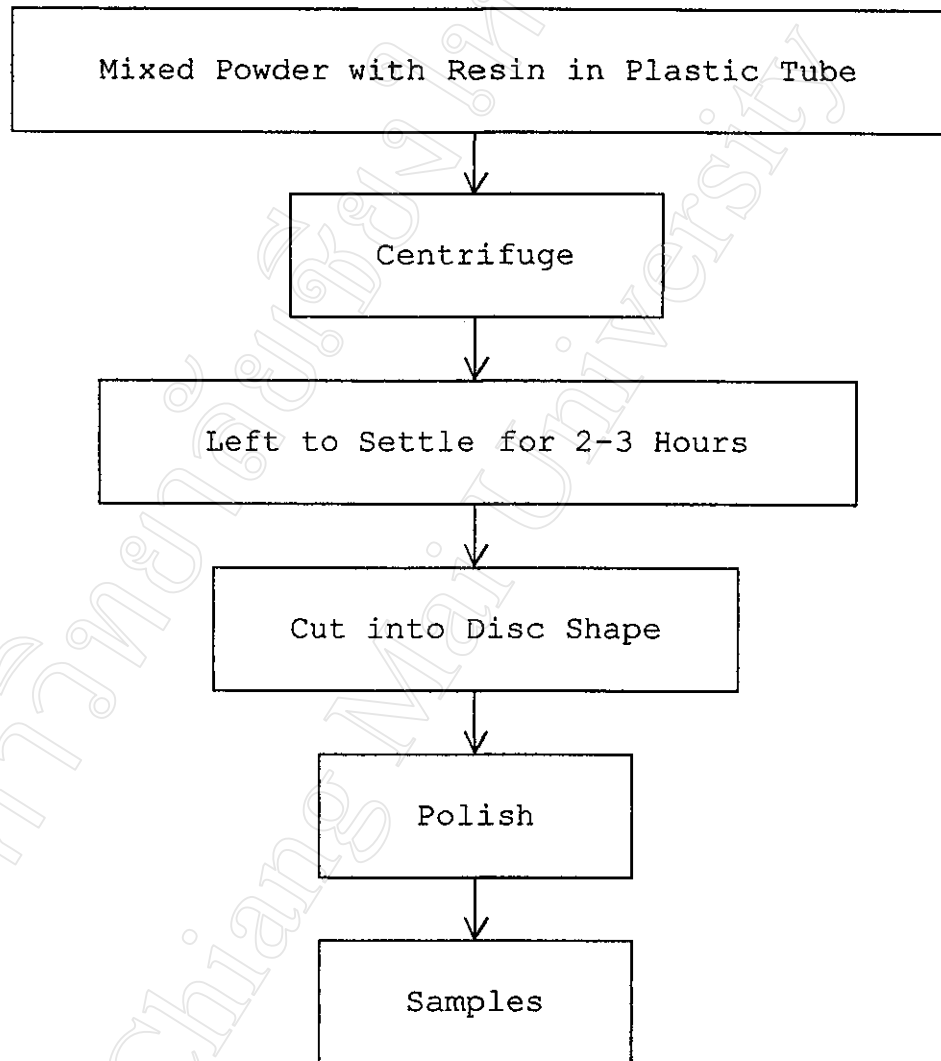


Figure 3.3 Schematic diagram of sample preparation using centrifuge method.

3.3 Characterization and Measurement Methods

3.3.1 Particle Size Analysis of PZT Powder

The particle size distribution of PZT powder was measured using a sedimentograph, and a scanning electron microscope. Fourier method was also employed to analyse the X-Ray diffracton line profiles to evaluate the particle size. Each method will be described in the next subsections.

3.3.1.1 Sedimentograph

The sieved PZT powder was dispersed in the water in the sample holder of Shimazu sedimentograph (model Analysette 22). Distribution curves representing the culmulative mass percent of particles with equivalent spherical diameters and the arithmetic mean of the particle size were shown in the next chapter.

3.3.1.2 Scanning Electron Microscopy

The particle size and morphology of the PZT ceramic powder and the microstructure of composites were characterized using scanning electron microscopy (SEM). The samples were mounted on metal sample holders prior to be coated with gold via r-f sputtering techniques. For PZT powder, they were dissolved in ethanal, shaken by ultrasonic bath, dropped the mixture on metal sample holder, left it dry in the air and then coated with gold.

3.3.1.3 Fourier Analysis

The x-ray line broadening produced in PZT powder was analyzed by the Fourier method to estimate the particle size and microstrain. The (111) interplanar spacing was selected. The sample annealed at 1300 °C was used as the standard to estimate the contribution of the instrument broadening. The measured line profiles were corrected for the instrumental broadening by the deconvolution method of

Stokes². The Fourier coefficients were analyzed by the procedure of Warren and Averbach³.

If \mathbf{s} is the reciprocal space vector given by $S = 2\sin\theta/\lambda$, and $\mathbf{s} = \mathbf{S} - \mathbf{r}$, where $r = 1/d$ and d is the spacing between atomic planes. Let $i_1(s)$, $i_0(s)$ and $i(s)$ be the observed profiles for the broadened samples, the standard and true profile of the line, respectively. The profile of the broadened sample is the convolutions of the true profile of the line and the profile of the standard; that is,

$$i_1(s) = i(s) * i_0(s) \quad (3.1)$$

and

$$\text{transf } i_1(s) = \text{transf } i(s) * \text{transf } i_0(s) \quad (3.2)$$

where the Fourier transform of $i_0(s)$ and $i_1(s)$ are

$$I_0(t) = \int i_0(s) \exp(2\pi jst) ds \quad (3.3)$$

and

$$I_1(t) = \int i_1(s) \exp(2\pi jst) ds \quad (3.4)$$

where $t = nd$ and n is integer

The $I_0(t)$ can separate into the real part and imaginary part as

$$I_{0re}(t) = \int i_0(s) \cos(2\pi st) ds \quad (3.5)$$

$$I_{0im}(t) = \int i_0(s) \sin(2\pi st) ds \quad (3.6)$$

These can be written as summations:

$$I_{0re}(t) = \sum i_0(s) \cos(2\pi st) \quad (3.7)$$

$$I_{0im}(t) = \sum i_0(s) \sin(2\pi st) \quad (3.8)$$

Now as $S = 2\sin\theta/\lambda$, $\Delta S = s = \cos\theta\Delta 2\theta/\lambda$, and then

$$\cos(2\pi st) = \cos[(2\pi t/\lambda) \cdot \cos\theta_{cen} \cdot (2\theta_i - 2\theta_{cen})] \quad (3.9)$$

and similarly for $\sin(2\pi st)$

$$\sin(2\pi st) = \sin[(2\pi t/\lambda) \cdot \cos\theta_{cen} \cdot (2\theta_i - 2\theta_{cen})] \quad (3.10)$$

where θ_{cen} is the centroid angle of the peak.

Hence,

$$I_{ore}(t) = \frac{\sum_{i=1}^N i_{0i} \cos[(2\theta_i - 2\theta_{cen}) \cdot \cos\theta_{cen} \cdot 2\pi t/\lambda]}{\sum_{i=1}^N i_{0i}} \quad (3.11)$$

$$I_{0im}(t) = \frac{\sum_{i=1}^N i_{0i} \sin[(2\theta_i - 2\theta_{cen}) \cdot \cos\theta_{cen} \cdot 2\pi t / \lambda]}{\sum_{i=1}^N i_{0i}} \quad (3.12)$$

which is similar to $I_1(t)$ in Eq. (3.2). The Fourier component of the true profiles is then

$$I(t) = \frac{I_1(t)}{I_0(t)} \quad (3.13)$$

As $I_0(t)$ and $I_1(t)$ are both complex, therefore

$$\begin{aligned} I(t) &= \frac{I_{ire}(t) + jI_{lim}(t)}{I_{0re}(t) + jI_{0im}(t)} \\ &= \frac{[I_{ire}(t) + jI_{lim}(t)] \cdot [I_{0re}(t) - jI_{0im}(t)]}{[I_{0re}(t)]^2 + [I_{0im}(t)]^2} \end{aligned} \quad (3.14)$$

whence

$$I_{re}(t) = \frac{I_{ire}(t) I_{0re}(t) + I_{lim}(t) I_{0im}(t)}{I_{0re}^2(t) + I_{0im}^2(t)} \quad (3.15)$$

and

$$I_{im}(t) = \frac{I_{lim}(t) I_{0re}(t) - I_{ire}(t) I_{0im}(t)}{I_{0re}^2(t) + I_{0im}^2(t)} \quad (3.16)$$

where $I_{re}(t)$ and $I_{im}(t)$ are the real part and the imaginary part of true Fourier component, respectively.

The initial slope of the curve of a plot of Fourier coefficient $I_{re}(t)$ as the function of t gives the particle size.³

The corrected shape of the peak is represented by a cosine Fourier series

$$I_{re}(n) = \langle \cos 2\pi l Z_n \rangle_{av} \approx \exp[-2\pi^2 l^2 \langle Z_n^2 \rangle] \quad (3.17)$$

where l is the peak value and Z_n is the relative displacements. The column length, L , and the change in length of the column, ΔL , are given by

$$L = nd, \quad \Delta L = dZ_n \quad (3.18)$$

The Z_n values are computed using Eq.(3.17). So, the strain for the respective direction is the initial slopes of the curve of a plot of ΔL vs L .

3.3.2 X-Ray Diffraction Analysis

The PZT powder was characterized by x-ray diffraction (JEOL) to determine the phase and interplanar spacing (hkl). The particle size of the powder was

measured employing Fourier analysis. X-ray diffraction examination was conducted using $\text{CuK}\alpha$ radiation through a Ni filter. The generator was operated at 30 kV and 20 mA. The XRD line profiles of the calcined PZT powder were obtained over a 2θ range of 20° - 60° , with a step of 0.5 degree and 1 sec counting time. In order to study the phase evolution with temperatures, the powder was annealed at temperatures of 1100°C , 1125°C , 1150°C , 1175°C and 1200°C , 1 hour each step. The peaks (100) and (001) were employed to study the changing of phase. For Fourier analysis, ball-milled powder was calcined at temperature range of 400°C - 1200°C , at a step of 100°C . The (111) peak was chosen to study the variation of the particle size. The data obtained from X-ray diffraction line profiles of this peak were stored into the computer program in order to determine the particle size and microstrain of the PZT powder.

3.4 Property Measurement of the Composites

3.4.1 Density Measurement

The density of the composite sample was measured using the Archimedes principle. The polished composite samples were first weighed in the air (W_d). Then, they were heated in boiling water for 10 min. After that, the samples were weighed again in pure water to determine the wet weights (W_w) by suspending on a thin copper wire. The density was then calculated from the following formula

$$\rho = \left(\frac{W_d}{W_d - W_w} \right) \cdot \rho_{\text{water}} \quad (3.19)$$

The theoretical density of the composite was also calculated. The following equation was used to determine volume% of ceramic loading of the composites.⁴

$$\rho_{\text{composite}} = (\text{vol}\% \text{ceramic}) \cdot \rho_{\text{ceramic}} + (\text{vol}\% \text{polymer}) \rho_{\text{polymer}} \quad (3.20)$$

3.4.2 Polarization of the Composites

The composites were polished to a thickness of 0.4-0.5 mm and electroded for poling with and air-dried silver paint (Archeson: ELECTRODAG 1415M). Guarded electrode was employed to avoid current shorting across the edges of the thin samples during the poling process. The electrodes were applied through a circle mask by the brush and allowed to dry at room temperature for 2 hours before poling.

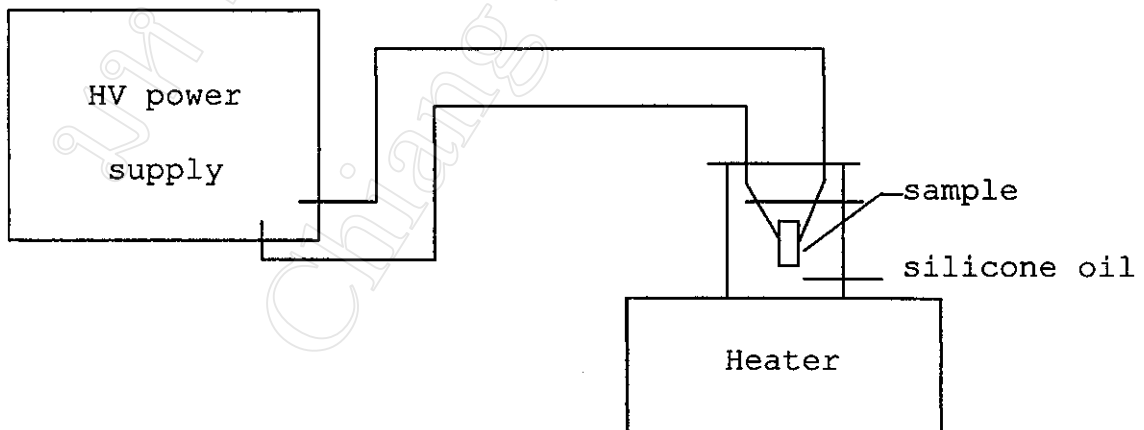


Figure 3.4 The poling apparatus.

Figure 3.4 shows a diagram of the poling apparatus which consists of a spring-loaded sample holder suspended in a temperature-controlled silicone oil bath and a dc high voltage generator. The voltage was applied stepwise, the specimen was held at a particular voltage for 3-5 minutes, and the field was then increased. This procedure minimized the possibility of dielectric breakdown and allowed higher fields to be applied. The maximum poling field was about 8-10 kV/mm at temperature of 70°C for 30 minutes.

3.4.3 Dielectric Properties

The capacitance (C) and dissipation factor ($\tan\delta$) of composites were measured at room temperature at a frequency range of 100-20,000 Hz using LCZ meter (Hewlett Packard : model 4276). The dielectric constant was determined from the equation,

$$\epsilon_r = Ct/\epsilon_0A \quad (3.21)$$

where

C is the sample capacitance,
t is the sample thickness,
 ϵ_0 is the permittivity of free space constant
(8.854×10^{-12} Farad per meter), and
A is the electroded area

3.4.4 Piezoelectric Properties

The piezoelectric charge coefficient (d_{33}) was measured dynamically using a Berlincourt Piezo d_{33} meter (model CADT) at a frequency of 100 Hz. The composite samples were put in the probes and the d_{33} values were read directly from meter display. The piezoelectric voltage coefficient (g_{33}) was then calculated using the relation

$$g_{33} = d_{33} / (\epsilon_r \epsilon_0) \quad (3.22)$$

3.4.5 Electromechanical Properties

The piezoelectric ceramic-polymer composites are known to exhibit a broadened nature of their resonance spectra. Thus, the conventional measurement technique to determine the electromechanical properties using the spectrum of impedance and frequency are difficult to apply on these composites. In this study, the electromechanical properties of 0-3 composites were determined from the measurement of the frequency spectra of capacitance (C) and conductance (G) using an impedance/gain phase analyzer (HP 4194A).

From IRE (now IEEE) standard on piezoelectric measurements⁵, the most important parameters for calculating these constants are the series and parallel resonance frequencies f_s and f_p , the geometric capacitance C_0 , and the minimum impedance $|Z_m|$ at resonance. An analyzer was used in measuring frequencies f_m and f_n corresponding to minimum and maximum impedance. In the presence of high mechanical losses, f_m and f_n are quite different from f_s and f_p . These results are shown in Figures 3.5 and 3.6. The IRE standard recommends that

$$\Delta f = (f_p - f_s) \approx \frac{f_n - f_m}{\left(1 + \frac{4}{M^2}\right)^{1/2}} \quad (3.23)$$

where the figure of merit M is given by

$$M = \frac{1}{2\pi f_s R_1 C_0} \approx \frac{1}{2\pi f_m (C_0 + C_1) |Z_m|} \quad (3.24)$$

where C_0 , C_1 are the capacitance of the parallel and series branches, respectively and R_1 is the resistance of the series branch of the equivalent circuit of the piezoelectric material near resonance. The sum $(C_0 + C_1)$ is the static capacitance, which was measured at a frequency well below fundamental resonance (for instance at 1 kHz).

The planar coupling coefficient k_p was calculated from the relation⁵

$$k_p^2 = \frac{\Delta f}{f_m} \left[\frac{R_1^2 - (1 - \sigma^2)}{1 + \sigma} \right] \quad (3.25)$$

where σ is the Poisson's ratio of the material, approximately 0.3 for PZT-resin composite and the value of R_1 is 2.05.

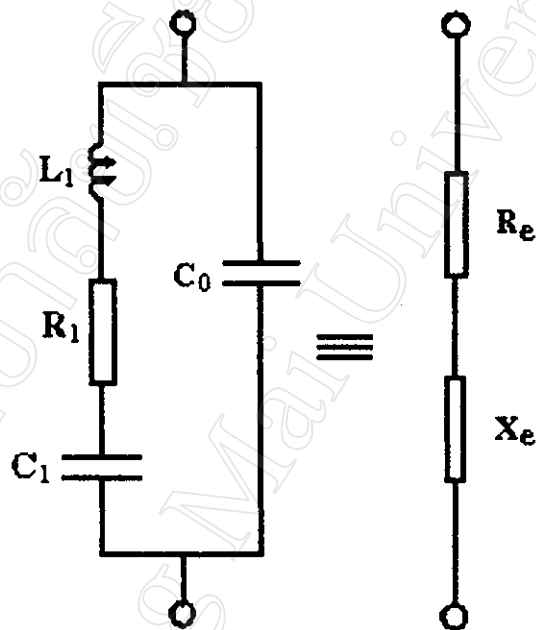
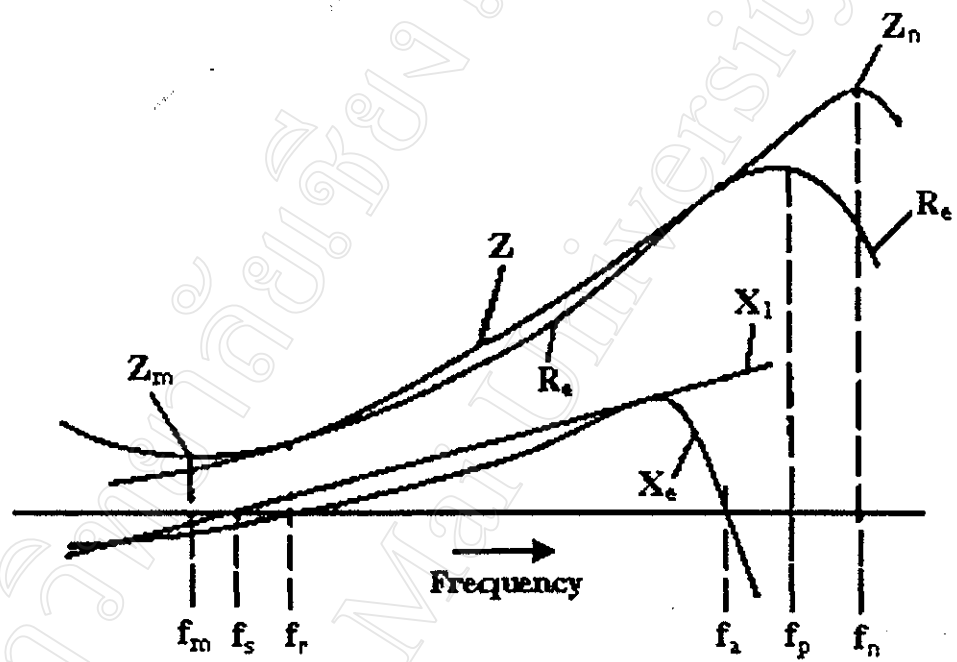


Figure 3.5 Equivalent circuit of the piezoelectric Material⁶.



- f_r, f_2 : reactance $X_e = 0$
 f_s : series arm reactance $X_1 = 0$
 f_p : resistive component $R_e = \max$
 f_m, f_n : impedance $Z = \min$ and \max

Figure 3.6 The frequency profiles of resonance mode of the piezoelectric material⁶.

The mechanical quality factor Q_m can be measured from the relation⁵

$$\frac{1}{Q_m} = 4\pi\Delta f|Z_m|(C_0 + C_1) \quad (3.26)$$

3.4.6 Acoustic Impedance

It is well known that the piezoelectric ceramic materials such as PZT with high electromechanical coupling suffer from a severe disadvantage when operated with a low impedance load such as that of the human body or water⁷. The acoustic impedance of PZT is around 30 Mrayl while that of the tissues is 1.5 Mrayl. Thus, this value is an important parameter of transducer.

The acoustic impedance (Z) of a material is related to its mechanical properties by the equation

$$Z = c_L\rho = (K\rho)^{0.5} \quad (3.27)$$

where c_L is the longitudinal velocity in the material, ρ and K are the material's density and Bulk Modulus,

respectively. The unit of Z is Mrayl (10^6 kg/sec.m^2) and K is N/m^2 .

The echo shift method⁸ is used to measure the longitudinal velocity in the samples. The equipment is shown in Figure 3.7. The pulse signals which generated from pulse generator were transmitted passing through the sample and reflected at the surface of a stainless steel target back to a receiver. The time shift (ΔT) in the echo is determined using the phase analyzer. The velocity was then calculated using the equation

$$c_L = 2t/\Delta T \quad (3.28)$$

where t is the thickness of the samples.

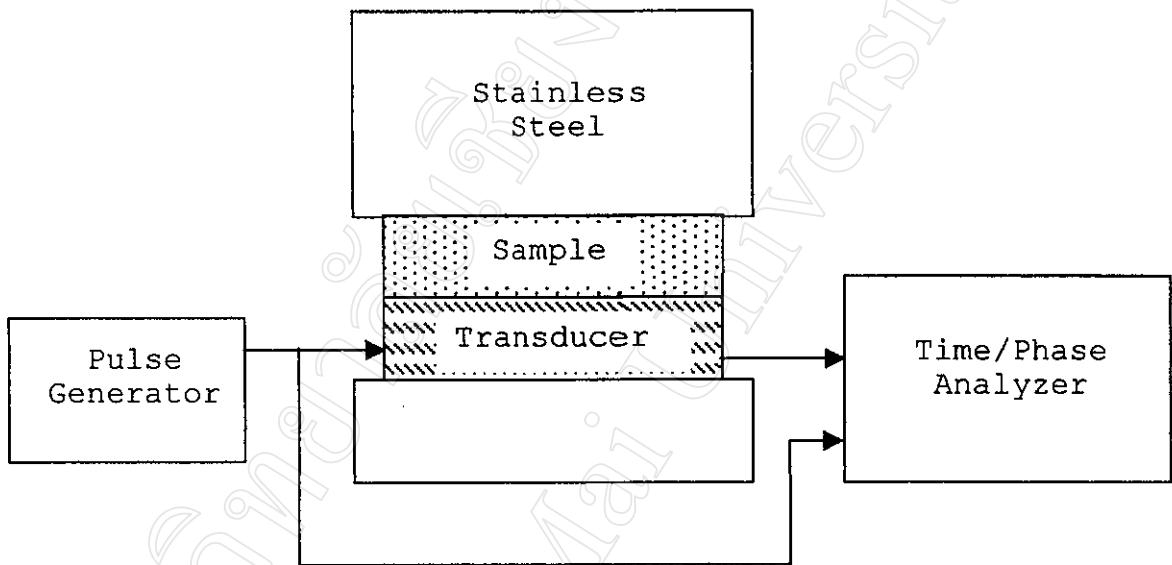


Figure 3.7 Diagram of the apparatus for echo shift measurement.

REFERENCES

1. W. Nhuapeng and T. Tunkasiri, *J. Am. Ceram. Soc.*, **85** [3] (2002).
2. A.R. Stokes, *Proc. Phys. Soc.*, **61**, 382 (1948).
3. B.E. Warren and B.L. Averbach, *J. Appl. Phys.*, **2**, 21 (1950).
4. K.H. Han, R.E. Riman and A. Safari, *J. Am. Ceram. Soc.*, 227-234 (1990).
5. "IRE Standards on Piezoelectric Crystals: Measurement of Piezoelectric Ceramics", *Proc. IRE*, **49**, 1161-1169 (1961).
6. A.J. Moulson and J.M. Herbert, "Electroceramics : Materials, Properties, and Applications" (Chapman and Hall, 1990) p.273.
7. T.R. Gururaja, W.A. Schulze, L.E. Cross, R.E. Newnham, B.A. Auld and Y.J. Wang, *IEEE Trans. Sonics Ultrasonics*, **SU-32**, 489-497 (1985).
8. T. Bui and H.L.W.C.T. Unsworth, *J. Acoust. Soc. Am.*, **83**, 2416- 2421 (1988).